Genetic characterization of glucose transporter function in *Leishmania mexicana*

Richard J. S. Burchmore*, Dayana Rodriguez-Contreras†, Kathleen McBride†, Michael P. Barrett*, Govind Modi‡, David Sacks‡, and Scott M. Landfear†§

*Institute of Biomedical and Life Sciences, Division of Infection and Immunity, Joseph Black Building, University of Glasgow, Glasgow G12 8QQ, United Kingdom; ‡Laboratory of Parasitic Diseases, National Institutes of Health, Bethesda, MD 20892; and †Department of Molecular Microbiology and Immunology, Oregon Health Sciences University, 3181 Southwest Sam Jackson Park Road, Portland, OR 97201

Both insect and mammalian life cycle stages of *Leishmania mexicana* take up glucose and express all three isoforms encoded by the *LmGT* glucose transporter gene family. To evaluate glucose transporter function in intact parasites, a null mutant line has been created by targeted disruption of the *LmGT* locus that encompasses the *LmGT1*, *LmGT2*, and *LmGT3* genes. This Δ*lmgt* null mutant exhibited no detectable glucose transport activity. The growth rate of the Δ*lmgt* knockout in the promastigote stage was reduced to a rate comparable with that of WT cells grown in the absence of glucose. Δ*lmgt* cells also exhibited dramatically reduced infectivity to macrophages, demonstrating that expression of LmGT isoforms is essential for viability of amastigotes. Furthermore, WT *L. mexicana* were not able to grow as axenic culture form amastigotes if glucose was withdrawn from the medium, implying that glucose is an essential nutrient in this life cycle stage. Expression of either *LmGT2* or *LmGT3*, but not of *LmGT1*, in Δ*lmgt* null mutants significantly restored growth as promastigotes, but only *LmGT3* expression substantially rescued amastigote growth in macrophages. Subcellular localization of the three isoforms was investigated in Δ*lmgt* cells expressing individual LmGT isoforms. Using anti-LmGT antiserum and GFP-tagged LmGT fusion proteins, LmGT2 and LmGT3 were localized to the cell body, whereas LmGT1 was localized specifically to the flagellum. These results establish that each glucose transporter isoform has distinct biological functions in the parasite.

The *Leishmania* species include human pathogens whose digenetic life cycle involves transmission of an extracellular flagellated promastigote from the gut of a hematophagous sandfly vector to a mammalian host, where the parasite multiplies within macrophage phagolysosomes as a nonmotile amastigote form. The two life cycle stages are exposed to highly contrasting nutritional environments. Sandflies feed principally on sugar-rich plant fluids and thereby subject promastigotes to high levels of sugars (1). When a sandfly ingests a bloodmeal containing *Leishmania* amastigotes, the parasites transform into promastigotes and multiply in the midgut. As the infection progresses, promastigotes colonize the insect foregut, where a subpopulation differentiates to metacyclic promastigotes that are highly motile and infective to mammals (2). Ingestion of a sugar-rich meal by the sandfly is required for successful transmission by bite (3), possibly because material released from the sugar crop (4) provides the major nutrient source in the cuticle-lined foregut (5).

On transmission to mammalian tissues, metacyclic promastigotes can survive phagocytosis by macrophages and multiply as amastigotes in a phagolysosome. This compartment is very acidic and will thus present special challenges to parasite membrane transporters (6). The phagolysosome is rich in the products of macromolecular breakdown but may not accumulate high levels of free glucose. *Leishmania* parasites down-regulate glucose transport activity (7) and up-regulate catabolism of fatty acids (8) as they transform from promastigote to amastigote, suggesting that uptake systems are developmentally regulated to maximize nutrient availability despite changing environments.

A gene family (*LmGT*) from *Leishmania mexicana* that encodes three distinct glucose transporter isoforms, LmGT1, LmGT2, and LmGT3, has been cloned recently (9). The LmGT glucose transporter isoforms are members of the major facilitator superfamily, a group of transport proteins (10) that mediate facilitated and active transport of various nutrients in both prokaryotes and eukaryotes. The amino acid identity among the LmGT isoforms is high, although discrete patches of divergence are clustered at the N and C termini and at several internal locations. mRNA derived from each of the *LmGT* genes is expressed in both promastigotes and amastigotes, although *LmGT2* mRNA is strongly up-regulated in promastigotes (9). The simultaneous presence of multiple glucose transporters might be explained by postulating discrete functions for each permease. In mammals, multiple hexose transporters exhibit different substrate specificities and have specific tissue and subcellular localizations commensurate with their biological roles. In *Leishmania*, the changing environments encountered by the parasite during its life cycle may require differential expression of glucose transporter isoforms. Moreover, the glycolytic enzymes responsible for glucose metabolism are sequestered in peroxisome-like organelles called glycosomes (11), implying a potential role for glucose translocation across the glycosomal membrane. A *Leishmania enriettii* glucose transporter isoform is localized to the flagellar membrane (12) for reasons that appear enigmatic because the glycosomes, and hence glycolysis, are probably restricted to the cell body. However, transporters and transporter-like proteins may have roles other than simply acquiring substrates for metabolism. For example, GLUT1, the archetypal mammalian glucose transporter, has a glucose-sensing function (13), and in yeast a number of transporter-like molecules have been shown to play roles in nutrient sensing (14). In the current study, we have investigated the biological function of the *L. mexicana* glucose transporters by generating a null mutant of the *LmGT1*, *LmGT2*, *LmGT3* gene cluster by targeted gene replacement (15). We have analyzed phenotypes of this glucose transporter "knockout" line, Δ*lmgt*, and of this null mutant complemented with each of the individual glucose transporter genes. The results reveal distinct roles for each transporter isoform and suggest important functions for these permeases in both promastigotes and amastigotes.
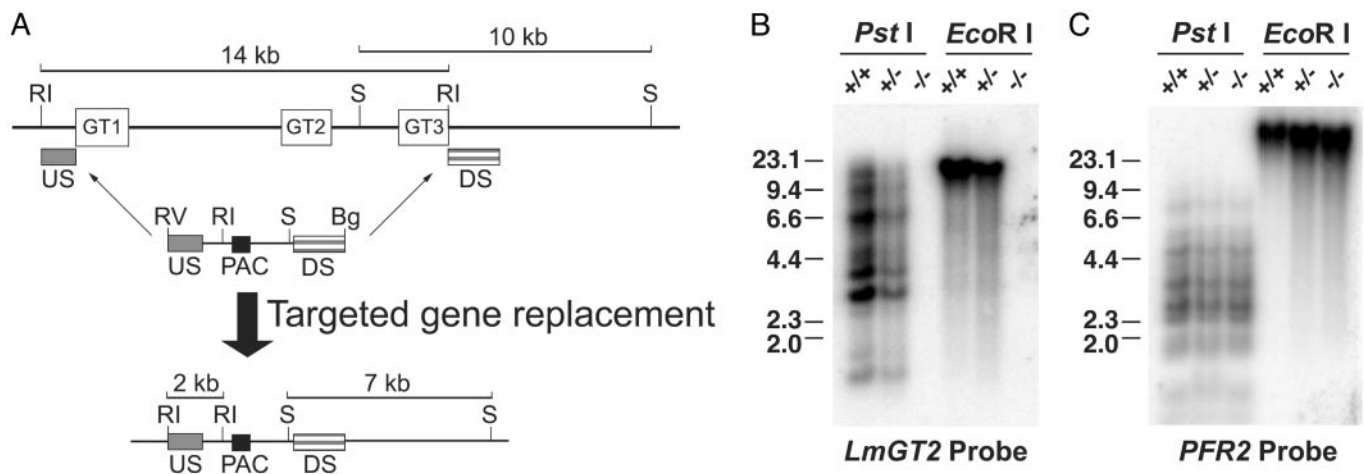
Materials and Methods

Parasite Culture. *L. mexicana* WT MNYC/BZ/62/M379 promastigotes were cultured at 26°C in MEM designated HOMEM (16), RPMI medium 1640, or DMEM-*Leishmania* [DME-L (17)], supplemented with 10% heat-inactivated FCS (iFCS). Culture

BIOCHEMISTRY

Fig. 1. Construction of the glucose transporter null mutant, Δ*lmgt*, by targeted gene replacement. (*A*) Strategy for targeted gene replacement. (*Upper*) The *LmGT* gene locus including the three ORFs (open rectangles marked GT1, GT2, and GT3), the 10-kb *Sma*I and 14-kb *Eco*RI restriction fragments, and the location of the upstream (US) and downstream (DS) segments used to target homologous recombination of the gene disruption constructs. One of these disruption constructs is shown immediately below the *LmGT* locus and includes the US and DS segments, the ORF for the PAC selectable marker, the *Eco*RV and *Bgl*II terminal polylinker restriction sites, and the internal *Eco*RI and *Sma*I restriction sites. The thin arrows indicate the sites of homologous integration. (*Lower*) The targeted gene replacement event is indicated below the thick arrow, showing the structure of the resulting chromosomal locus and the predicted 2-kb *Eco*RI and 7-kb *Sma*I restriction fragments that are diagnostic of the correct homologous integration event. Symbols indicating restriction fragments are: RI, *Eco*RI; S, *Sma*I; RV, *Eco*RV; and Bg, *Bgl*II. Generation of the null mutant required a second targeted gene replacement using a similar gene disruption cassette containing a SAT marker. (*B*) Southern blot containing 10 μg of genomic DNA from WT parasites (+/+), heterozygous knockout line after integration of the PAC gene disruption construct (+/−), or Δ*lmgt* null mutant (−/−) digested with *Pst*I or with *Eco*RI and hybridized with a radiolabeled probe representing the *LmGT2* ORF. The numbers indicate the positions and sizes (kilobase pairs) of DNA molecular weight markers. (*C*) The same blot shown in *B* after elution of the *LmGT2* probe and rehybridization to the *PFR2* probe that encodes an unrelated paraflagellar rod protein.

form (CF) amastigotes (9) were grown at 32.5°C in either Schneider's *Drosophila* medium or in DME-L containing 30 mM Mes buffer instead of Hepes. Both of these media were supplemented with 20% iFCS and were adjusted to pH 5.5.

Infection of Cultured Peritoneal Macrophages. Peritoneal exudate macrophages were isolated from female BALB/c mice by peritoneal lavage, seeded onto chamber slides at a density of 2×10^5 per ml, and incubated overnight in RPMI at 32°C, 5% CO_2. Attached macrophages were washed with fresh RPMI, then incubated for 6 h with stationary phase promastigotes at 2×10^5 per ml in RPMI at 32°C, 5% CO_2. Residual free parasites were removed by three washes with RPMI, and slides were incubated as above in RPMI until fixation. Slides were fixed with methanol, stained with Giemsa, and examined under the microscope to detect intracellular parasites.

Generation of the Δ*lmgt* Line. *LmGT* alleles were replaced sequentially with puromycin acetyltransferase (PAC) and streptothricin acetyltransferase (SAT) genes, encoding resistance markers for the antibiotics puromycin and nourseothricin, respectively. The gene deletion construct for puromycin selection (LmGTKOPAC) was based on the *Leishmania* expression vector pX63PAC (18). Flanking sequences upstream (1.2 kb) of the *LmGT1* ORF and downstream (1.8 kb) of the *LmGT3* ORF (upstream and downstream segments, respectively; Fig. 1*A*) were amplified by PCR, using primers that incorporated restriction sites suitable for subsequent insertion into the polylinker regions flanking the PAC gene in pX63PAC. The gene deletion construct for nourseothricin selection (LmGTKOSAT) was generated by removing the PAC coding region from LmGTKOPAC and replacing it with a fragment containing the SAT coding region from pCPC-SAT (19). Plasmid DNA for each construct was digested with three restriction enzymes to destroy the plasmid backbone, and the linear gene deletion constructs were gel purified by using QIAEX columns (Qiagen, Valencia, CA).

L. mexicana promastigotes were grown in culture to $\approx 8 \times 10^6$ per ml, washed in cold Zimmerman medium with glucose (ZMG) (20) and resuspended in cold ZMG at 1×10^8 per ml. Four hundred-microliter aliquots were electroporated with ≈ 5 μg of linear DNA (0.45 kV, 500 μF by using a Bio-Rad Gene Pulser II apparatus) in 0.2 cm of electrode gap cuvettes, transferred to 5 ml of HOMEM/10% iFCS, and incubated at 26°C. After 24 h, cells were pelleted and resuspended in 5 ml of fresh HOMEM/10% iFCS with puromycin at 10 μg/ml or nourseothricin at 25 μg/ml. When living cells were observed (after ≈ 10 days in a typical experiment), clones were derived by limiting dilution on multiwell plates, without allowing further expansion of the initial drug-resistant population. Multiple cloned lines were picked and inoculated into larger volumes of HOMEM/10% iFCS with selective drug(s) for characterization of the integrations by genomic Southern blotting.

After the first round of targeting, puromycin-resistant clones were analyzed by Southern blot to select a clone that had the desired integration (i.e., replacement of one *LmGT* allele). One such clone (Fig. 1*B*) was chosen for the second round of targeting, and puromycin selection was maintained through all subsequent manipulations. Multiple double drug-resistant clones were obtained after the second round of targeting. For some of these clones, Southern blot analysis revealed that both alleles of the LmGT cluster were deleted. One of these clones was selected for further study.

Uptake Assays. Assays for uptake of [³H]D-glucose, [¹⁴C]D-glucose, [³H]2-deoxy-D-glucose, and [³H]adenosine in *L. mexicana* promastigotes were performed essentially as reported (21). For substrate saturation curves of LmGT2 and LmGT3, incubations with [¹⁴C]D-glucose were performed for 20 s, after pilot studies indicated that uptake was linear for at least this period over the range of glucose concentrations used. For LmGT1, uptake assays were performed with [³H]glucose between 0 and 50 s, and the initial rate data were fitted to a straight line by linear regression.

Infection of Sandflies with Promastigotes. Three- to five-day-old *Lutzomyia longipalpis* sandflies were fed through a chick-skin membrane on a mixture of heparinized mouse blood containing $1–4 \times 10^6$ procyclic promastigotes per ml, obtained from 1- to 2-day-old logarithmic cultures. Blood-engorged sandflies were separated and maintained at 28°C with 30% sucrose solution. At various times after feeding, the flies were anesthetized with CO_2, and their midguts were dissected and examined microscopically for the presence and location of promastigotes. The number of midgut promastigotes was determined by placing individual midguts into a microcentrifuge tube containing 30 μl of PBS, pH 7.4, homogenizing each gut by using a Teflon-coated micro-tissue grinder, and counting released promastigotes in a hemacytometer.

Preparation of Peptide Antiserum. Synthesis of a peptide (CSSLS-GNRAE) encompassing the COOH-terminal nine amino acids of LmGT1 and LmGT2 and containing a NH_2-terminal cysteine residue, coupling to keyhole limpet hemocyanin, and generation of rabbit polyclonal antisera were performed by Alpha Diagnostic International (San Antonio, TX). Crude antiserum was affinity-purified by using the cognate peptide coupled to Affigel 15 (Bio-Rad), following the manufacturer's instructions. Affinity-purified antiserum was used at a 1:50 dilution.

Fluorescence Microscopy. The $\Delta lmgt$ cells expressing LmGT1 or LmGT2 were processed for immunofluorescence microscopy by using affinity-purified primary antibody and fluorescein isothiocyanate-coupled goat anti-rabbit secondary antibody, as described (22). For expression of proteins consisting of GFP fused to the COOH terminus of LmGT2 or LmGT3, each transporter ORF was subcloned into the pX-'GFP expression vector (23). Fluorescence images of $\Delta lmgt$ cells expressing LmGT2-GFP and LmGT3-GFP were obtained as described (24). Fluorescence and differential interference contrast images were obtained and deconvolved by using the Deltavision Image Restoration System (Applied Precision Instruments, Issaquah, WA).

Results

Targeted Replacement of the LmGT1, LmGT2, LmGT3 Gene Cluster. To determine the biological function(s) of the *L. mexicana* glucose transporters LmGT1, LmGT2, and LmGT3, knockout parasites were created by double-targeted gene replacement of the *LmGT* locus (Fig. 1*A*). A clonal line representing the doubly disrupted null mutant of the *LmGT* locus, designated $\Delta lmgt$, was examined by Southern blot analysis to demonstrate that the correct homologous integration had occurred. Genomic DNA from the $\Delta lmgt$ line ($-/-$, Fig. 1*B*) did not hybridize to a probe from the *LmGT2* ORF that hybridizes to all three *LmGT* genes (9), whereas DNA from WT *L. mexicana* or from the heterozygous knockout line ($+/+$ and $+/-$, respectively, Fig. 1*B*) did hybridize to this probe, demonstrating that all three *LmGT* ORFs had been eliminated from the $\Delta lmgt$ line. Probing the Southern blot with the paraflagellar rod gene, *PFR2* (25), revealed hybridization to DNA from all three cell lines (Fig. 1*C*). Furthermore, hybridization with the upstream probe demonstrated that a 14-kb *Eco*RI fragment present in DNA from WT parasites was reduced to a predicted band of 2 kb, whereas hybridization with the downstream probe revealed that a 10-kb *Sma*I band in WT DNA was reduced in size to a predicted band of 7 kb (Fig. 1*A* and data not shown). Together, these results confirm that the correct homologous integrations had occurred at the 5' and 3' sides of the *LmGT* locus for both rounds of homologous gene replacement.

Transport Properties of $\Delta lmgt$ Knockout Promastigotes. To determine the transport phenotype of the $\Delta lmgt$ null mutants, uptake assays were performed on both WT and $\Delta lmgt$ cells by using the
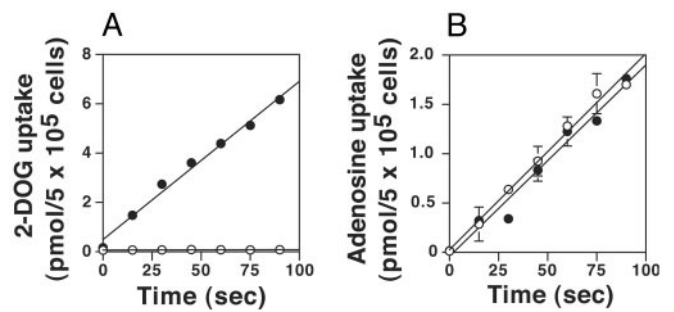
Fig. 2. Uptake of [³H]2-deoxy-D-glucose (2-DOG, *A*) and [³H]adenosine (*B*) by WT (filled circles) and $\Delta lmgt$ null mutant (open circles) parasites. The error bars in this and other figures indicate the SD.

glucose analog [³H]2-deoxy-D-glucose (Fig. 2*A*). WT cells exhibited robust uptake, whereas the $\Delta lmgt$ cells were incapable of taking up the glucose analog. In contrast, both cell lines incorporated [³H]adenosine at identical rates (Fig. 2*B*), indicating that the null mutants were competent for transport of adenosine. These results imply that *LmGT1*, *LmGT2*, and *LmGT3* are probably the only functional glucose transporter genes in *L. mexicana*.

Growth Properties of $\Delta lmgt$ Promastigotes. To determine the role of the LmGT transporters in parasite growth, we examined the growth of WT and $\Delta lmgt$ promastigotes in DME-L medium (17) with and without 25 mM glucose and with and without 5 mM proline, an amino acid that can be used as an alternative energy source by *Leishmania* promastigotes (26). In medium containing both glucose and proline, $\Delta lmgt$ parasites grew less rapidly and to a lower cell density than WT cells, doubling from 1×10^7 to 2×10^7 cells per ml in ≈ 60 h compared with ≈ 20 h for WT cells and attaining a density of $\approx 2.5 \times 10^7$ cells per ml compared with $\approx 5 \times 10^7$ cells per ml for WT cells [compare WT(+G, +P) to $\Delta lmgt$(+G, +P), Fig. 3]. The growth rate of $\Delta lmgt$ cells was unaffected by withdrawal of glucose from the culture medium [compare $\Delta lmgt$(+G, +P) to $\Delta lmgt$(−G, +P), Fig. 3*B*]. In contrast, WT parasites grew more slowly in medium without glucose compared with medium containing glucose [compare WT(+G, +P) to WT(−G, +P), Fig. 3*A*]. Notably, WT cells in glucose-deficient medium had the same growth rate as $\Delta lmgt$ cells growing in either the presence or absence of glucose. Thus, either removal of glucose from the medium [WT(−G, +P), Fig. 3*A*] or elimination of glucose transport capacity [$\Delta lmgt$(+G, +P), Fig. 3*B*] slowed parasite growth to the same extent compared with WT cells grown in the presence of glucose. In
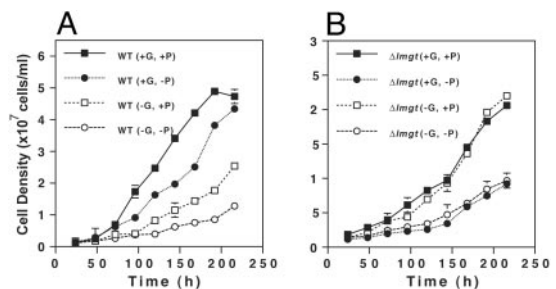
Fig. 3. Growth of WT (*A*) and $\Delta lmgt$ (*B*) promastigotes in DME-L medium containing (+) or lacking (−) 25 mM glucose (G) or 5 mM proline (P). Parasites were inoculated at an initial density of 1×10^6 cells per ml, and aliquots of the cultures were counted ($n = 3$, average $\pm$ SD) on a hemacytometer at various times thereafter.

BIOCHEMISTRY
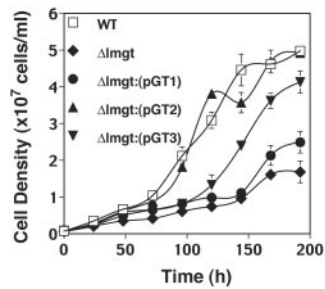
Fig. 4. Growth in RPMI medium of promastigotes of WT, Δ*lmgt* null mutant, and Δ*lmgt* null mutants complemented with each of the *LmGT* genes (Δ*lmgt*[*pGT1*], Δ*lmgt*[*pGT2*], Δ*lmgt*[*pGT3*]).

Fig. 5. Infection of *L. longipalpis* sandflies by WT (filled circles) and Δ*lmgt* (open circles) promastigotes. At each time point after infection, midguts were dissected from 10–12 sandflies, and parasites were quantitated. Similar results were obtained from four independent experiments.
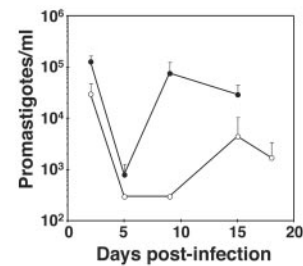
summary, glucose uptake promotes growth of WT promastigotes but is not essential for survival.

Similarly, we have determined that removal of proline from the medium further slows growth of both WT and Δ*lmgt* parasites in either the presence or absence of glucose (compare +P and −P curves in Fig. 3). Hence, consistent with previous observations by others (27), both glucose and proline can support growth of promastigotes and, in the absence of glucose uptake, proline can function as a major source of energy. Although Δ*lmgt* cells grow very slowly in the absence of both glucose and proline, they are still viable and probably use other amino acids as energy sources (28), albeit inefficiently.

Ability of Individual LmGT Isoforms to Promote Growth of Promastigotes. To assess the role of each LmGT isoform in supporting growth of promastigotes, we complemented the Δ*lmgt* null mutant individually with the *LmGT1*, *LmGT2*, or *LmGT3* ORF and monitored growth in RPMI containing 25 mM glucose. A region of each gene containing the ORF was subcloned into the *Leishmania* expression vector pX63NEO (29) and transfected into the Δ*lmgt* line to generate the Δ*lmgt*[*pGT1*], Δ*lmgt*[*pGT2*], and Δ*lmgt*[*pGT3*] lines, each of which was complemented with the gene for one isoform. Growth curves (Fig. 4) revealed that the *LmGT2* gene was able to complement growth of the null mutant to the same level as WT parasites. *LmGT3* was able to partially restore the growth rate, but *LmGT1* provided very little increase in growth over the level of the Δ*lmgt* null mutant.

Growth of Δ*lmgt* Promastigotes in Sandflies. Glucose is thought to be an important nutrient for the promastigote in the sandfly and has been proposed to be essential for development of infectious parasites in the insect (3). To determine whether the glucose uptake is important for parasite growth in the sandfly, we infected *L. longipalpis* with both WT and Δ*lmgt* knockout parasites and monitored the number of parasites in the insect midgut as a function of time (Fig. 5). WT parasites established initial infections with ≈10^5 parasites per midgut, which then dropped to ≈10^3 parasites during excretion of the blood meal on day 5, followed by repopulation of the midgut, including the anterior midgut, by day 9. In contrast, Δ*lmgt* parasites grew significantly less efficiently in the midgut, especially after excretion of the bloodmeal, and the repopulation occurred later (day 15) and to a lesser extent than for WT parasites.

Development of Metacyclic Promastigotes in WT and Δ*lmgt* Parasites. To determine whether deletion of the glucose transporter genes affects transformation of *L. mexicana* promastigotes into infectious metacyclic forms whose abundance is increased in stationary-phase promastigote cultures (2) and in the anterior of the sandfly during a natural infection (30), we monitored metacyclogenesis in stationary-phase cultures by Percoll density gradi-

ent enrichment (31) followed by morphological quantitation (32). WT parasites produced 7.8% and 10.4% metacyclic forms in two cultures, whereas Δ*lmgt* parasites produced 2.5% metacyclic forms in both cases. Furthermore the *meta 1* transcript, which is up-regulated in metacyclic parasites (33), was induced 3.6-fold in WT stationary-phase compared with mid-logarithmic phase parasites, whereas the transcript was induced 1.7-fold in stationary-phase Δ*lmgt* cells. By these criteria, metacyclogenesis appears to be impaired but not abrogated in glucose transporter null mutants.

Growth of the Δ*lmgt* Null Mutant and Individual Complemented Lines as Amastigotes. To determine whether glucose transporters play a significant role in the amastigote stage of the life cycle, we infected macrophages with WT and Δ*lmgt* null mutant cells (Fig. 6). Primary cultures of mouse peritoneal exudate cells, which are comprised chiefly of macrophages (34), were exposed to infection by stationary-phase WT and Δ*lmgt* cells. After 6 h of exposure similar numbers of intracellular parasites were observed (≈10–15 parasites per 100 macrophages), indicating that each cell line possessed a similar capacity to infect macrophages (data not shown). However, 48 h after infection, only 1% of macrophages examined harbored Δ*lmgt* amastigotes, whereas 26% of macrophages harbored WT parasites. Six days after infection, 1% of macrophages were infected with Δ*lmgt* cells, whereas 35% were infected with WT parasites, and 182 WT parasites were observed per 100 macrophages examined, compared with two Δ*lmgt* parasites per 100 macrophages. These
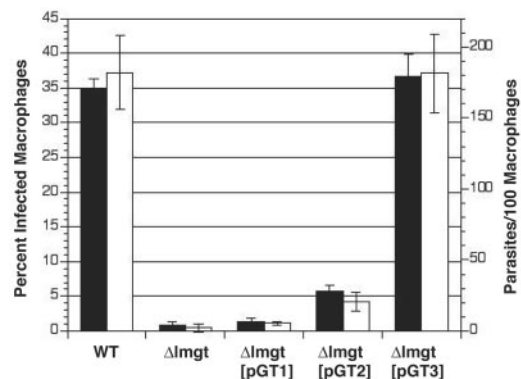
Fig. 6. Growth of WT, Δ*lmgt*, Δ*lmgt*[*pGT1*], Δ*lmgt*[*pGT2*], and Δ*lmgt*[*pGT3*] lines in murine peritoneal macrophages. Filled bars represent percent of infected macrophages, and open bars represent parasites per 100 macrophages for the same fields. Primary peritoneal macrophages were infected with stationary phase promastigotes, and the number of intracellular amastigotes (n = 3, average ± SD) was quantitated 6 days after infection.
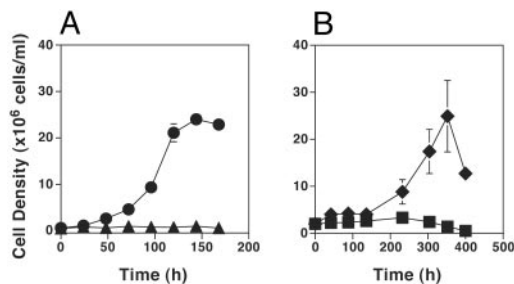
Fig. 7. Growth of WT *L. mexicana* and Δ*lmgt* null mutants as axenic CF amastigotes. (*A*) WT (circles) and Δ*lmgt* (triangles) parasites were inoculated into Schneider's medium supplemented with 20% iFCS and adjusted to pH 5.5 followed by incubation at 32.5°C, and aliquots were withdrawn and counted (*n* = 3, average ± SD) at various times. (*B*) CF amastigotes of WT *L. mexicana*, growing in DME-L medium containing 30 mM Mes buffer, pH 5.5, and supplemented with 20% iFCS (CF-DME-L), were pelleted, washed, and inoculated at a density of 1 × 10⁶ cells per ml into fresh CF-DME-L constituted with 11 mM glucose and dialyzed iFCS (diamonds), or CF-DME-L deficient in glucose and constituted with dialyzed iFCS (squares).

results, repeated in three independent experiments, indicate that survival of Δ*lmgt* cells in macrophages is dramatically reduced, suggesting that glucose transport is essential for amastigote viability. To address the possibility that LmGT isoforms might differ in their ability to promote amastigote survival, we performed similar studies with the Δ*lmgt*[*pGT1*], Δ*lmgt*[*pGT2*], and Δ*lmgt*[*pGT3*] individually complemented lines. Strikingly, expression of *LmGT1* gave no significant rescue of amastigote growth, whereas *LmGT2* restored growth to a small degree, but expression of *LmGT3* was sufficient to rescue growth to levels comparable with WT. Because the number of intracellular parasites for all cell lines studied was similar after 6 h of infection, *LmGT3* expression seem to be important for survival in the parasitophorous vacuole rather than for uptake of the parasite into macrophages. Additional experiments performed by using J774G8 macrophage-like host cells (35) gave similar results, except that the level of amastigote growth restoration by complementation with *LmGT2* was more variable, and in one case reached ≈40% the number of amastigotes present in WT or *LmGT3* complemented null mutants. Furthermore, when macrophages were infected with WT *L. mexicana* expressing each isoform fused to GFP, fluorescence from each isoform was observed in the membranes of intracellular amastigotes (data not shown). Hence the failure of *LmGT1* and *LmGT2* to efficiently restore growth of amastigotes was not due to failure of the corresponding proteins to be expressed in amastigotes.

Growth of WT and Δ*lmgt* Parasites as CF Amastigotes. To determine whether amastigotes require glucose uptake for viability, thus potentially explaining the failure of Δ*lmgt* parasites to survive inside macrophages, we have grown both WT and Δ*lmgt* null mutant parasites as axenic CF amastigotes (9, 36), allowing the nutrient content of the medium to be manipulated. Similar to the macrophage infections discussed above, WT parasites grew robustly as CF amastigotes, whereas Δ*lmgt* null mutants did not grow (Fig. 7*A*). Furthermore, WT *L. mexicana* grew robustly as CF amastigotes in medium containing 11 mM glucose and dialyzed iFCS, but deletion of glucose from the synthetic medium coupled with its removal from iFCS by dialysis resulted in failure of the parasites to grow (Fig. 7*B*). Consequently, *L. mexicana* apparently require glucose to survive as amastigotes, and the nonviability of the Δ*lmgt* null mutants, either inside macrophages (Fig. 6) or as CF amastigotes (Fig. 7*A*), is likely due to their failure to take up this essential nutrient.

Characterization of Glucose Transport by Each Isoform. To define the glucose-transport characteristics of each LmGT isoform, transport assays were performed with the Δ*lmgt*[*pGT1*], Δ*lmgt*[*pGT2*], and Δ*lmgt*[*pGT3*] lines. Substrate saturation curves for uptake of [¹⁴C]glucose were generated for each line and revealed apparent K_m values for D-glucose of 1.22 ± 0.22 mM, 109 ± 28 μM, and 208 ± 40 μM for LmGT1, LmGT2, and LmGT3, respectively (*n* = 3). Thus LmGT1 is a lower-affinity glucose transporter than LmGT2 or LmGT3.

Subcellular Localization of the LmGT1, LmGT2, and LmGT3 Transporters. To determine whether the isoforms might also differ in subcellular localization, we defined the distribution of each protein by deconvolution fluorescence microscopy. In the first approach, an antiserum was raised against the peptide CSSLS-GNRAE that encompasses the last nine amino acids of LmGT1 and LmGT2, which differ from those of LmGT3 (9). A negative control sample of Δ*lmgt* cells showed only diffuse staining over the body of the cells using this antiserum. The immunofluorescence images (Fig. 8 *A* and *B*, which is published as supporting information on the PNAS web site, www.pnas.org) clearly indicate that LmGT1 is localized primarily in the flagellum, whereas LmGT2 is targeted to the pellicular plasma membrane (12) that surrounds the cell body.

To define the location of LmGT3 and to provide another reagent to confirm the location of LmGT2, we also prepared fusion constructs in which GFP (37) was fused to the COOH terminus of each of these two isoforms. Deconvolution fluorescence images of cells expressing LmGT2-GFP (Fig. 8*C*) and LmGT3-GFP (Fig. 8*D*) revealed that both of these proteins are located largely on the pellicular plasma membrane that surrounds the cell body and found only at very low levels on the flagellum. Furthermore, studies on the uptake of [³H]2-deoxy-D-glucose by using the Δ*lmgt*[*pGT2-GFP*] and Δ*lmgt*[*pGT3-GFP*] lines confirmed that these fusion proteins are functional glucose transporters (data not shown) and thus are not significantly disrupted by fusion to GFP.

Discussion

In many organisms, including kinetoplastid parasites, multiple glucose transporters are coexpressed, and functional characterization of individual glucose transporter isoforms has depended on separate expression in heterologous systems such as *Xenopus* oocytes. However, a "gold standard" for assessing the biological function of each gene in an organism is to generate a "knockout" line and to examine the phenotype of this null mutant. To assess the phenotype of *L. mexicana* without glucose transporters and to functionally evaluate each of the three LmGT isoforms in a null background, we have generated a *LmGT* knockout line. Δ*lmgt* promastigotes were unable to take up radiolabeled glucose, confirming that members of the LmGT family are responsible for glucose uptake in promastigotes. The reduced growth rate, but continued viability, of Δ*lmgt* promastigotes supports existing biochemical evidence that glucose is a major but not exclusive source of metabolic energy for *Leishmania* promastigotes. These results are further confirmed by the observation that Δ*lmgt* promastigotes grow poorly in the sandfly *L. longipalpis* and thus establish an important, albeit not essential, role for the parasite glucose transporters in the infection of the insect vector.

Functional characterization reveals important differences between the three LmGT isoforms in relation to glucose transport and ability to support parasite growth in both promastigotes and amastigotes. Expression of individual *LmGT* genes in Δ*lmgt* promastigotes revealed that expression of *LmGT2* is sufficient to completely restore the WT growth phenotype. This result is consistent with the observation that *LmGT2* mRNA is strongly up-regulated in WT promastigotes (9), and LmGT2 may be the isoform that is responsible for most of promastigote glucose

uptake. Expression of *LmGT3* was sufficient to partially restore the growth of Δ*lmgt*, but *LmGT1* gave only very limited growth restoration, although both of these transcripts are present constitutively throughout the life cycle. These observations are consistent with the functional characterization of the three LmGT isoforms, because LmGT2 and LmGT3 are glucose transporters with relatively high affinity, whereas LmGT1 by comparison is a lower-affinity glucose transporter.

In addition to the functional differences described above, subcellular localization studies indicate that LmGT1 is a flagellar protein, whereas both LmGT2 and LmGT3 are pellicular plasma membrane isoforms. These results are similar to those previously obtained with the two related glucose transporter isoforms from *L. enriettii*, in which ISO1 was demonstrated to be a flagellar transporter and ISO2 a pellicular plasma membrane permease (12, 38). Although LmGT1 is closely related to LmGT2 and LmGT3 in primary structure and predicted membrane topology, it bears a large NH$_2$-terminal hydrophilic extension that is predicted to have an intracellular orientation and might play a role in restricting cell surface localization, as is the case for the ISO1 glucose transporter in *L. enriettii* (12).

The distinct subcellular distributions of the different isoforms suggest the possibility of biologically significant functional specializations that may be associated with the divergent targeting of each permease. It is noteworthy that in other organisms, axoneme-containing organelles such as flagella and cilia are often involved in environmental sensing (39). Hence, one possible explanation for the flagellar localization of LmGT1 is that it might function as a glucose sensor. Furthermore, in other organisms such as *Saccharomyces cerevisiae* (40), *Neurospora crassa* (41), and humans (13), glucose transporter-like proteins have been shown to function as glucose sensors. Whether LmGT1 functions as a glucose sensor may be an important topic of future investigations.

A significant role for glucose transporters in amastigotes is revealed by the observation that the Δ*lmgt* line was unable to sustain infection in murine peritoneal exudate cells. These results imply that glucose transporter expression is essential for amastigote viability and were unanticipated, given that glucose uptake (7) and catabolism (42) are thought to be down-regulated in amastigotes. Furthermore, the failure of Δ*lmgt* null mutants to grow as CF amastigotes and the inability of WT parasites to survive as CF amastigotes in medium devoid of glucose further imply that glucose is an essential nutrient for amastigotes and that glucose transporter null mutants are not viable as amastigotes for this reason. The ability of LmGT3, but not of LmGT1 or LmGT2, to fully restore WT viability suggests that LmGT3 may subsume an essential role in the parasitophorous vacuole. This environment is not well understood, but free glucose levels in macrophage phagolysosomes may be low. Thus LmGT3 might function in the amastigote to scavenge sparse glucose from the lumen of the parasitophorous vacuole. Regardless of their precise roles in amastigote biochemistry, the apparent requirement of amastigotes for functional glucose transporters raises the possibility that interference with parasite glucose transporter function might be of therapeutic value in *L. mexicana* infections and that these permeases could be targets for drug development.

Although it is clear that glucose is a nonessential nutrient for promastigotes in axenic culture, glucose transport may be critical to *Leishmania* development in the sandfly host. The diet and digestive physiology of the sandfly is not well understood, but a substantial body of evidence suggests that sugars in the sandfly diet are important in the development of *Leishmania* promastigotes into infectious forms (reviewed in ref. 43). The significantly reduced numbers of parasites in the anterior midgut of sandflies infected with the Δ*lmgt* null mutants would very likely reduce the competence of these vectors to transmit an infection to the vertebrate host.

1. Anez, N., Luga, A., Loaiza, A., Nieves, D. & Orozco, J. (1994) *Med. Vet. Entomol.* **8,** 38–42.
2. Sacks, D. L. & Perkins, P. V. (1984) *Science* **223,** 1417–1419.
3. Schlein, Y. (1986) *Parasitol. Today* **2,** 175–177.
4. Tang, Y. & Ward, R. D. (1988) *Med. Vet. Entomol.* **12,** 13–19.
5. Richards, A. G. (1975) *Acta Trop.* **32,** 83–95.
6. Burchmore, R. J. S. & Barrett, M. P. (2001) *Int. J. Parasitol.* **31,** 1311–1320.
7. Burchmore, R. J. S. & Hart, D. T. (1995) *Mol. Biochem. Parasitol.* **74,** 77–86.
8. Hart, D. T. & Coombs, G. H. (1982) *Exp. Parasitol.* **54,** 397–409.
9. Burchmore, R. J. S. & Landfear, S. M. (1998) *J. Biol. Chem.* **273,** 29118–29126.
10. Pao, S. S., Paulsen, I. T. & Saier, M. H. (1998) *Microbiol. Mol. Biol. Rev.* **62,** 1–34.
11. Michels, P. A. M., Hannaert, V. & Bringaud, F. (2000) *Parasitol. Today* **16,** 482–489.
12. Piper, R. C., Xu, X., Russell, D. G., Little, B. M. & Landfear, S. M. (1995) *J. Cell Biol.* **128,** 499–508.
13. Bandyopadhyay, G., Sagan, M. P., Kanoh, Y., Standaert, M. L., Burke, T. R., Quon, M. J., Reed, B. C., Dikic, I., Noel, L. E., Newgard, C. B., *et al.* (2000) *J. Biol. Chem.* **275,** 40817–40826.
14. Johnston, M. (1999) *Trends Genet.* **15,** 29–33.
15. Cruz, A., Coburn, C. M. & Beverley, S. M. (1991) *Proc. Natl. Acad. Sci. USA* **88,** 7170–7174.
16. Berens, R. L., Brun, R. & Krassner, S. M. (1976) *J. Parasitol.* **62,** 360–365.
17. Iovannisci, D. M. & Ullman, B. (1983) *J. Parasitol.* **69,** 633–636.
18. Freedman, D. J. & Beverley, S. M. (1993) *Mol. Biochem. Parasitol.* **62,** 37–44.
19. Bart, G., Frame, M. J., Carter, R., Coombs, G. H. & Mottram, J. C. (1997) *Mol. Biochem. Parasitol.* **88,** 53–61.
20. Carruthers, V. B., van der Ploeg, L. H. T. & Cross, G. A. M. (1993) *Nucleic Acids Res.* **10,** 2537–2538.
21. Seyfang, A. & Landfear, S. M. (2000) *J. Biol. Chem.* **275,** 5687–5693.
22. Snapp, E. L. & Landfear, S. M. (1999) *J. Biol. Chem.* **274,** 29543–29548.
23. Ha, D. S., Schwarz, J. K., Turco, S. J. & Beverley, S. M. (1996) *Mol. Biochem. Parasitol.* **77,** 57–74.
24. Vasudevan, G., Ullman, B. & Landfear, S. M. (2001) *Proc. Natl. Acad. Sci. USA* **98,** 6092–6097.
25. Moore, L. M., Santrich, C. & LeBowitz, J. H. (1996) *Mol. Biochem. Parasitol.* **80,** 125–135.
26. ter Kuile, B. H. (1993) *Parasitol. Today* **9,** 206–210.
27. Krassner, S. M. & Flory, B. (1971) *J. Parasitol.* **57,** 917–920.
28. Glew, R. H., Saha, A. K., Das, S. & Remaley, A. T. (1988) *Microbiol. Rev.* **52,** 412–432.
29. LeBowitz, J. H., Coburn, C. M. & Beverley, S. M. (1991) *Gene* **103,** 119–123.
30. Sacks, D. L., Hieny, S. & Sher, A. (1985) *J. Immunol.* **135,** 564–569.
31. Späth, G. F. & Beverley, S. M. (2001) *Exp. Parasitol.* **99,** 97–103.
32. Bates, P. A. & Tetley, L. (1993) *Exp. Parasitol.* **76,** 412–423.
33. Nourbakhsh, F., Uliana, S. R. B. & Smith, D. F. (1996) *Mol. Biochem. Parasitol.* **76,** 201–213.
34. Mottram, J. C., Souza, E. A., Hutchison, J. D., Carter, R., Grame, M. J. & Coombs, G. H. (1996) *Proc. Natl. Acad. Sci. USA* **93,** 6008–6013.
35. Chang, K.-P. (1980) *Science* **209,** 1240–1242.
36. Pan, A. (1984) *Exp. Parasitol.* **58,** 72–80.
37. Stauber, R. H., Horie, K., Carney, P., Hudson, E. A., Tarasova, N. I., Gaitnaris, G. A. & Pavlakis, G. N. (1998) *BioTechniques* **24,** 462–471.
38. Snapp, E. L. & Landfear, S. M. (1997) *J. Cell Biol.* **139,** 1775–1783.
39. Landfear, S. M. & Ignatushchenko, M. (2001) *Mol. Biochem. Parasitol.* **115,** 1–17.
40. Özcan, S., Dover, J., Rosenwald, A. G., Wölf, S. & Johnston, M. (1996) *Proc. Natl. Acad. Sci. USA* **93,** 12428–12432.
41. Madi, L., McBride, S. A., Bailey, L. A. & Ebbole, D. J. (1997) *Genetics* **146,** 499–508.
42. Mukkada, A. J., Meade, J. C., Glaser, T. A. & Bonventre, P. F. (1985) *Science* **229,** 1099–1101.
43. Killick-Kendrick, R. (1979) in *Biology of Kinetoplastida*, eds. Lumsden, W. H. R. & Evans, D. A. (Academic, London), Vol. 2, pp. 395–460.